

Radiation propagation time broadening of the instrument response function in time-resolved fluorescence spectroscopy

Alexander A. Fedorov, Sandrina P. Barbosa, Mário N. Berberan-Santos *

Centro de Química-Física Molecular, Instituto Superior Técnico, PT-1049-001 Lisboa, Portugal

Received 27 December 2005; in final form 15 January 2006

Available online 9 February 2006

Abstract

It is shown that radiation propagation may affect time-resolved fluorescence measurements involving millimetre-sized systems and picosecond time scales. For this purpose, the effect of the excitation beam width on the instrument response function is studied. Experimental results for a scattering suspension of silica nanoparticles in a square 1 cm cell are analysed according to the developed model. The model accounts well for the observations, the retrieved parameters being in very good agreement with expectations.

© 2006 Elsevier B.V. All rights reserved.

1. Introduction

The space and time scales involved in most laboratory fluorescence measurements are such that it is appropriate to neglect the finiteness of the speed of light, which is approximately 0.30 mm/ps in a vacuum, and a little less in common solvents, e.g. 0.22 mm/ps in water for visible radiation (430 nm).

However, when dealing with very short time scales (femtoseconds, a few picoseconds) and/or extended laboratory systems (a few millimetres in linear dimension) in the picosecond range, the propagation time of radiation becomes of importance. In water, for instance, a difference in path-length of 1 mm corresponds to a time lag of about 5 ps, which may be nonnegligible when the goal is the measurement of short fluorescence lifetimes or events.

We have previously considered the effect of the time of flight of the photons in a mainly qualitative way in the context of atomic and molecular radiative transfer [1,2], and quantitatively for two specific time-resolved fluorescence excitation–detection geometries [3,4]. The model developed was successfully applied to systems with intermediate and long fluorescence lifetimes (Rhodamine 101 and coronene

solutions, respectively) and to a purely scattering system (suspension of silica nanoparticles), corresponding to the case of zero lifetime [3,4]. We also showed that from the time dependence of the recorded signal (fluorescence or back-scattered light) the absorption or scattering coefficient of the sensed medium can be determined [3].

In this work, we show that radiation propagation times cannot also be neglected in principle for millimetre-sized systems and picosecond time scales. For this purpose, the effect of the excitation beam width on the instrument response function is studied. Experimental results for a suspension of silica nanoparticles acting as the scattering medium are analysed according to the developed model. The model accounts well for the observations, the retrieved parameters being in very good accord with expectations.

2. Experimental

A square 1 cm cell was filled with a dilute aqueous suspension of silica nanoparticles (Ludox TM-50, Aldrich). The equivalent absorbance of the suspension at 430 nm was very low, 0.03, in order to avoid multiple scattering. A right angle geometry was used, as shown in Fig. 1. Time-resolved picosecond fluorescence measurements were performed using the single-photon timing method with laser excitation. The set-up consisted of a Spectra-Physics

* Corresponding author. Fax: +351 21 846 44 55.

E-mail address: berberan@ist.utl.pt (M.N. Berberan-Santos).

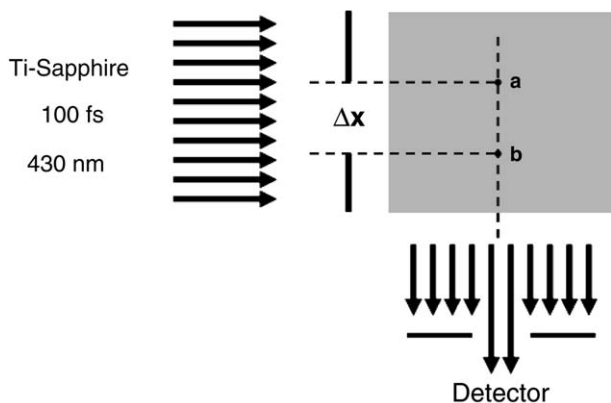


Fig. 1. Right angle geometry. The exciting radiation, with a flat intensity profile, passes through a slit Δx . The light scattered at point a has a delay $\Delta x/v$ with respect to excitation light scattered at point b . Multiple scattering is not considered.

Millenia Xs Nd:YVO₄ diode pumped laser, pumping a pulse picked Spectra-Physics Tsunami titanium-sapphire laser, delivering 100 fs frequency-doubled pulses at a repetition rate of 4 MHz. The wavelength selected after frequency doubling was 430 nm. The emission signal passed through a depolarizer, a Jobin-Yvon HR320 monochromator with a grating of 100 lines/nm and 1 mm slits, and was detected with a Hamamatsu 2809U-01 microchannel plate photomultiplier (MCP-PMT). A time scale of 0.65 ps/channel was used. The initial width (1.5 mm) of the excitation laser beam after frequency doubling was increased with lenses in order to obtain a flat horizontal intensity profile with a width of ca. 10 mm. An entrance slit placed before the cell, see Fig. 1, allowed to control the effective width Δx of the excitation beam entering the cell. The vertical dimension of the beam (6 mm) was essentially constant, i.e., after passing the entrance slit the beam cross section had a rectangular shape. Detection optics was such that only scattered photons coming from the center of the cell (less than 1 mm image size) were detected, see Fig. 1.

3. Theory

Suppose that the laser pulse duration is so brief that it approaches a delta function. Further assume that the laser pulse has a flat intensity profile with a width larger than the entrance slit Δx , cf. Fig. 1. The finite width of the entrance slit will necessarily broaden the excitation pulse, as there is a time difference $\Delta t = \Delta x/v$ (where v is the speed of light in the medium) between the photons scattered in points a and b , and collected at the detector, see Fig. 1. For an excitation beam with rectangular cross section and with a flat intensity profile, and for an optically thin scattering medium, the resulting outgoing pulse is a rectangular function $S(t)$ whose width is Δt , Fig. 2.

On the other hand, even for a narrow entrance slit, the recorded signal, the so-called instrument response function (IRF), is not a delta function, owing mainly to the temporal broadening contribution of the photomultiplier (transit

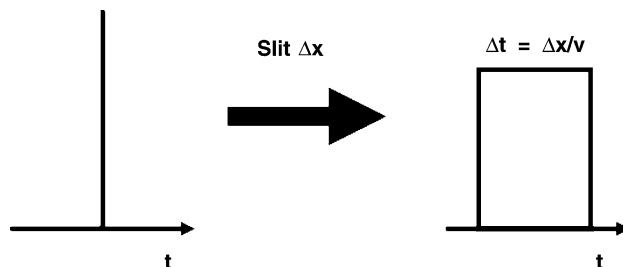


Fig. 2. Rectangular pulse as a result of propagation time broadening of a spatially extended delta pulse.

time spread, or TTS) [5–8], and in some apparatuses also to other contributions like the temporal broadening contribution of the diffraction grating monochromator [7–9]. For a narrow entrance slit, the IRF will be denoted $L_0(t)$. In this way, the observed IRF $L(t)$ for an entrance slit Δx will be

$$L(t) = S(t) \otimes L_0(t), \quad (1)$$

where \otimes stands for the convolution between two functions. The main effect is an additional broadening of the IRF.

Assuming that $L_0(t)$ is a Gaussian function, the effect of a finite slit Δx when $S(t)$ is narrower than $L_0(t)$ will be to broaden the Gaussian profile of the IRF, without significantly changing its shape. Only when the width of $S(t)$ approaches or exceeds that of $L_0(t)$ does the shape of $L(t)$ deviate significantly from the Gaussian shape.

It follows from Eq. (1) that the variance of $L(t)$ is

$$\sigma^2 = \sigma_0^2 + \sigma_S^2, \quad (2)$$

where σ_S is the standard deviation of $S(t)$ and σ_0 is the standard deviation of $L_0(t)$. For a rectangular distribution, the standard deviation is related to the width $\Delta t = \Delta x/v$ by

$$\sigma_S = \frac{1}{2\sqrt{3}} \frac{\Delta x}{v}. \quad (3)$$

One obtains from Eqs. (2) and (3) that

$$\sigma^2 = \sigma_0^2 + \frac{1}{12v^2} (\Delta x)^2. \quad (4)$$

Note that for a Gaussian function, the full width at half maximum (FWHM) is

$$\text{FWHM} = 2\sqrt{2 \ln 2} \sigma = 2.35\sigma, \quad (5)$$

where σ is the standard deviation.

4. Experimental results and discussion

Experimental IRFs were recorded for several entrance slits with the set-up described in Section 2. As shown in Fig. 3, the function $L(t)$ was always very close to a Gaussian, except for its far right wing (characteristic of most MCPs), which is irrelevant for our purposes. The standard deviation for each slit width was computed from the FWHM using Eq. (5). A plot of the variance σ^2 as a function of $(\Delta x)^2$ is shown in Fig. 4, and can be seen to follow a straight line (within experimental uncertainty), in agree-

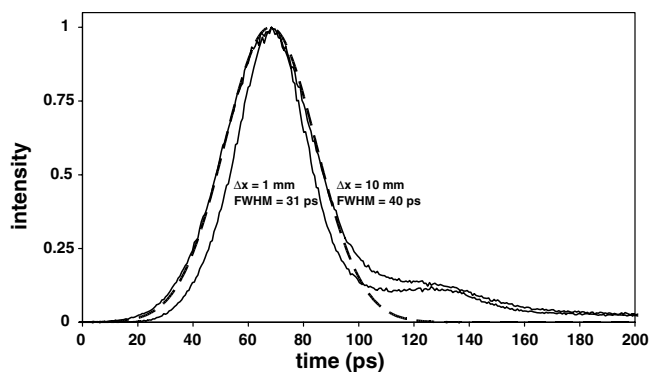


Fig. 3. Instrument response function (IRF) recorded for two extreme values of the entrance slit width, 1 and 10 mm. The IRF is practically Gaussian (dashed line) for all slit widths used.

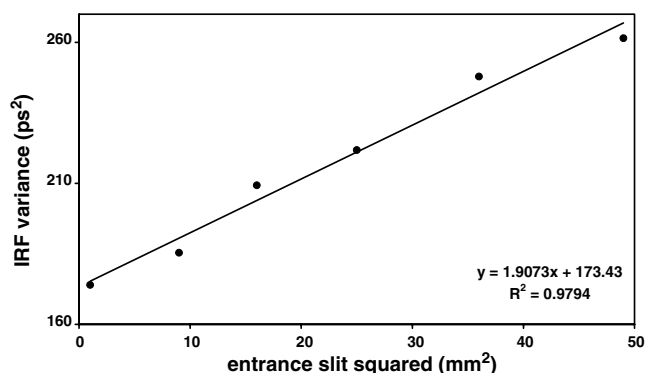


Fig. 4. Variance of the IRF as a function of the square of the slit width (for $\Delta x \leq 7$ mm). The full line is the linear regression result.

ment with Eq. (4). The point for $\Delta x = 10$ mm (not shown) is out of trend, owing to the beam profile edge effect.

From the intercept and slope one obtains, respectively, a minimum FWHM of 31 ± 1 ps, and a light speed of 0.21 ± 0.02 mm/ps. Both values are in good agreement with expectations. Indeed, from the refractive index of water at 430 nm and at 20 °C, $n = 1.3407$ [10,11], the computed speed of light is $v = c/n = 0.224$ mm/ps.

The FWHM dependence on slit width is not linear (except for very large Δx), as follows from Eqs. (4) and (5). This dependence is displayed in Fig. 5. The point for $\Delta x = 10$ mm is clearly out of trend for the above mentioned reasons. It is also seen that the FWHM increases noticeably with respect to the minimum value of 31 ps for a slit as narrow as 3 mm.

In this work, the effect of the entrance slit width on the IRF was studied. A similar study could have been carried out on the exit slit width instead. The results are expected to be similar whenever the area viewed by the monochromator entrance slit is several mm wide. In this case however, other factors may play a role, such as a change in the illuminated area of the photocathode with the slit width [7,9].

The results obtained show that radiation propagation times cannot in principle be neglected in millimetre-sized

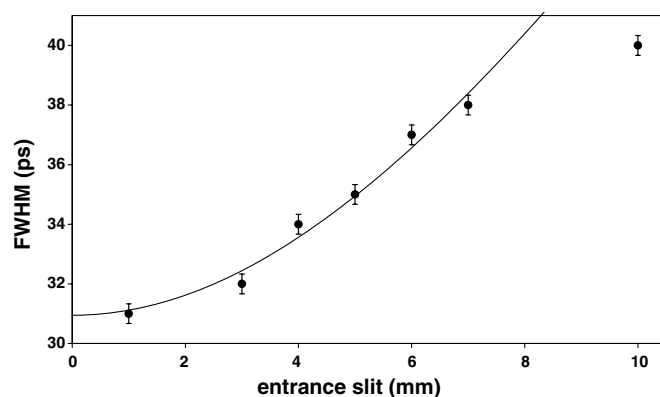


Fig. 5. Full width at half maximum (FWHM) as a function of the slit width. The full line is the fitted curve with the parameters obtained from Eq. (4).

systems for picosecond time scales. The importance of this contribution will be the more relevant, the narrower the IRF, hence the shorter the TTS of the MCP used, as follows from Eq. (4). MCPs with a TTS shorter than the current 25 ps FWHM for the fastest models may become available in the future, depending on technical improvements and market needs. A microchannel plate PMT with a TTS as short as 10 ps FWHM is reported to have been produced [12].

Another fast detector used in time-resolved fluorescence is the streak camera. With this type of detector it is possible to attain a resolution better than 500 fs in the accumulative mode [13,14]. The results obtained here are also relevant for measurements with streak camera detection, provided the experimental geometry corresponds to Fig. 1.

In fluorescence lifetime measurements, the usual procedure is to record the IRF at the excitation wavelength using a scattering solution, and then to measure the fluorescence decay of the sample at the emission wavelength. Radiation propagation time artifacts may occur whenever the solvents used in the two measurements have different refractive indexes, or when the optical densities or slits used differ in the two cases. The same applies to the alternative procedure of using a reference fluorophore. For the current MCPs, a laser beam width of 1.5 mm or less ensures nevertheless that no significant radiation propagation time broadening occurs, as shown in Fig. 5. This may not be the case when faster MCPs become available, or when streak cameras are used.

5. Conclusions

The effect of the finiteness of the speed of light on the instrument response function in fluorescence lifetime measurements was demonstrated quantitatively by studying the effect of the excitation beam width on the instrument response function. Experimental results for a dilute suspension of silica nanoparticles were analysed according to the developed model. The model accounts well for the observa-

tions, the retrieved parameters being in good accord with expectations.

Acknowledgement

This work was supported by Fundação para a Ciência e a Tecnologia (FCT, Portugal) within project POCTI/58535/QUI/2004.

References

- [1] M.N. Berberan-Santos, E.J. Nunes Pereira, J.M.G. Martinho, *J. Chem. Phys.* 103 (1995) 3022.
- [2] E.J. Nunes Pereira, J.M.G. Martinho, M.N. Berberan-Santos, *Phys. Rev. Lett.* 93 (2004) 120201.
- [3] S.P. Barbosa, A. Fedorov, M.N. Berberan-Santos, *Chem. Phys. Lett.* 406 (2005) 243.
- [4] S.P. Barbosa, A. Fedorov, M.N. Berberan-Santos, *J. Fluoresc.*, in press.
- [5] D. Beelaar, *Rev. Sci. Instrum.* 57 (1986) 1116.
- [6] H. Kume, K. Koyama, K. Nakatsugawa, S. Suzuki, D. Fatlowitz, *Appl. Opt.* 27 (1988) 1170.
- [7] N. Boens, in: W.R.G. Baeyens, D. De Keukeleire, K. Korkidis (Eds.), *Luminescence Techniques in Chemical and Biochemical Analysis*, Marcel Dekker, New York, 1991, p. 21.
- [8] G. Hungerford, D. Birch, *Meas. Sci. Technol.* 7 (1996) 121.
- [9] M. vandeVen, M. Ameloot, B. Valeur, N. Boens, *J. Fluoresc.* 15 (2005) 377.
- [10] X. Quan, E.S. Fry, *Appl. Opt.* 34 (1995) 3477.
- [11] P.D.T. Huibers, *Appl. Opt.* 36 (1997) 3785.
- [12] T. Credo, H. Frisch, H. Sanders, R. Schroll, F. Tang, in: *Proceedings of the Nuclear Science Symposium and Conference Recording vol. 1*, IEEE 2004, p. 586.
- [13] Hamamatsu Photonics, *Guide to Streak Cameras*, Hamamatsu City, 2002.
- [14] M.M. Shakya, Z. Chang, *Appl. Phys. Lett.* 87 (2005) 041103.